Electrochemical Properties of a Molecular Assembly Comprised of Multiple, Identical Interactive Redox Centers. Voltammetric Characterization of μ-Oxo-(tetra-*tert*-butylphthalocyaninato)silicon

David C. Gale and John G. Gaudiello*,†

Contribution from the Systems Technology Division, IBM Corporation, Endicott, New York 13760, and the Department of Chemistry and the Center for Fundamental Materials Research, Michigan State University, East Lansing, Michigan 48824. *Received May 21, 1990*

Abstract: The redox chemistry for the oxidation of the soluble polymer μ-oxo-(tetra-*tert*-butylphthalocyaninato)silicon and the corresponding dicapped monomer, bis(trimethylsiloxy)(tetra-*tert*-butylphthalocyaninato)silicon, were characterized by a variety of electrochemical techniques. The polymer exhibits a broad continuous oxidation process over a 1750-mV range while the monomer undergoes two Nernstian one-electron oxidations over the same potential region. Controlled-potential coulometry studies suggest that the polymer assembly can be oxidized to any fractional oxidation state ranging from 0 to 1+ and is chemically stable at all oxidation levels. Rotating disk, cyclic, and differential pulse voltammograms display a continuous redox response over the same potential range. The voltammograms are characteristic of Nernstian processes, suggesting that the broad current response is due to the through-space electronic interactions that are known to exist between the phthalocyanine rings. Comparison between the polymer and monomer results allows for a quantitative description of the voltammetry of the polymer. Digital simulations of the electrochemical responses indicate that the oxidation of the polymer can be modeled as a series of reversible redox couples in equilibrium undergoing sequential electron transfer. These results are used to estimate the amount of electronic interactions existing between the redox sites.

Introduction

The electrochemical properties of molecules that contain multiple, identical redox centers have been the subject of numerous studies.[1] The materials have ranged from soluble oligomers and polymers investigated in solution to electroactive sites anchored covalently or electrostatically to electrode surfaces. These studies have provided information concerning the potential required to access the different redox states, the rates of heterogeneous and homogeneous (both intra- and intermolecular) electron transfer, conformational changes accompanying the redox processes, the environment and mobility of the electroactive centers, and the amount of interaction between the redox sites. The potential, magnitude, and shape of the electrochemical response for both the soluble and surface-confined materials have been shown to be dependent on these effects.

For compounds comprised of multiple identical noninteractive redox centers, a single voltammetric response with a current-potential shape and potential equivalent to that of the corresponding monomer is predicted.[2] The magnitude of the current depends on the total number of electroactive sites and the formal potential of each pair of successive oxidation states is governed solely by statistical factors. A wide variety of soluble redox-active compounds and chemically modified electrodes exhibit voltammetric waves that have been accurately interpreted by employing this model.[1a,2,3]

Electrochemical studies of systems having substantial interactions between redox sites have been relatively rare.[4] Most studies have been of materials containing only several centers where individual redox processes are observed for each electroactive site. Various types of organometallic compounds have exhibited this type of mixed-valence behavior. The onset of the redox process becomes energetically more favorable as the degree of interaction and the number of sites increase. The delocalization of charge over the entire molecule stabilizes the redox product with respect to the monomer.[5]

One of the most widely studied classes of compounds that contain multiple interactive centers is the soluble silicon phthalocyanine oligomers.[6] These materials are comprised of phthalocyanine macrocycles (Pc) held in a cofacial orientation by an oxygen-silicon-oxygen backbone ($R_3SiO[Si(R'_4)PcO]_nSiR_3$, R = *n*-$C_6H_{13}$, $C(CH_3)_3$, CH_3; R' = H, C_8H_6; *n* = 1-4). The electrochemical,[6] spectroscopic,[7] and photoelectrochemical[8]

† Present address: IBM Corp., 1701 North St. Endicott, NY 13760.

(1) (a) For a review of chemically modified electrodes containing identical redox sites see: Murray, R. W. In *Electroanalytical Chemistry*; Bard, A. J., Ed.; Dekker: New York, 1984; Vol. 13, and references therein. (b) For compounds comprised of multiple, identical noninteractive redox sites, see: References 2 and 3. (c) For compounds comprised of multiple, identical interactive redox sites, see: Reference 4. (d) For compounds comprised of multiple, identical redox sites that are electrically conductive, see: Reference 7.

(2) Flanagan, J. B.; Margel, S.; Bard, A. J.; Anson, F. C. *J. Am. Chem. Soc.* **1978**, *100*, 4248-4253.

(3) (a) Smith, T. W.; Kuder, J. E.; Wychick, D. *J. Polym. Sci., Polym. Chem. Ed.* **1976**, *14*, 2433-2448. (b) Itaya, K.; Bard, A. J.; Szwarc, M. *Z. Phys.* **1978**, *112*, 1-9. (c) Saji, T.; Pasch, N. F.; Webber, S. E.; Bard, A. J. *J. Phys. Chem.* **1979**, *82*, 1101-1105. (d) Funt, B. L.; Hsu, L. C.; Hoang, P. M. *J. Polym. Sci., Polym. Chem. Ed.* **1981**, *19*, 203-211. (e) Funt, B. L.; Hsu, L. C.; Hoang, P. M.; Martenot, J. P. *J. Polym. Sci., Polym. Chem. Ed.* **1982**, *20*, 109-118. (f) Funt, B. L.; Hoang, P. M. *J. Electrochem. Soc.* **1984**, *131*, 2289-2298. (g) Fan, F.-R. F.; Mau, A.; Bard, A. J. *Chem. Phys. Lett.* **1985**, *116*, 400-404. (h) Kawai, T.; Iwakura, C.; Yoneyama, H. *Electrochim. Acta* **1989**, *34*, 1357-1361.

(4) (a) Morrison, W. H., Jr.; Krogsrud, S.; Hendrickson, D. N. *Inorg. Chem.* **1973**, *12*, 1998-2004. (b) Brown, G. M.; Meyer, T. J.; Cowan, D. O.; LeVanda, C.; Kaufman, F.; Roling, P. V.; Rausch, M. D. *Inorg. Chem.* **1975**, *14*, 506-511. (c) LeVanda, C.; Bechgard, K.; Cowan, D. O.; Rausch, M. D. *J. Am. Chem. Soc.* **1977**, *99*, 2964-2967. (d) Desbois, M. H.; Astruc, D.; Guillin, J.; Maroit, J. P.; Varret, F. *J. Am. Chem. Soc.* **1985**, *107*, 5280-5282, and references therein. (e) Van Order, N., Jr.; Geiger, W. E.; Bitterwolf, T. E.; Rheingold, A. L. *J. Am. Chem. Soc.* **1987**, *109*, 5680-5690, and references therein.

(5) Yap, W. T.; Durst, R. A. *J. Electroanal. Chem.* **1981**, *30*, 3-8.

(6) (a) Mezza, T. M.; Armstrong, N. R.; Ritter, G. W.; Iafalice, J. P.; Kenney, M. E. *J. Electroanal. Chem.* **1982**, *137*, 227-237. (b) Wheeler, B. L.; Nagasubramanian, G.; Bard, A. J.; Schechtman, L. A.; Dininny, D. R.; Kenney, M. E. *J. Am. Chem. Soc.* **1984**, *106*, 7404-7410. (c) DeWulf, D. W.; Leland, J. K.; Wheeler, B. L.; Bard, A. J.; Batzel, D. A.; Dininny, D. R.; Kenney, M. E. *Inorg. Chem.* **1987**, *26*, 260-270. (d) Simic-Glavaski, B.; Tanaka, A. A.; Kenney, M. E.; Yeager, E. *J. Electroanal. Chem.* **1987**, *229*, 285-296.

(7) (a) Janson, T. R.; Kane, A. R.; Sullivan, J. F.; Knox, K.; Kenney, M. E. *J. Am. Chem. Soc.* **1969**, *91*, 5210-5214. (b) Kane, A. R.; Sullivan, J. F.; Kenney, D. H.; Kenney, M. E. *Inorg. Chem.* **1970**, *9*, 1445-1448. (c) Hush, N. S.; Woolsey, I. S. *Mol. Phys.* **1971**, *21*, 465-474. (d) Mooney, J. R.; Choy, C. K.; Knox, K.; Kenney, M. E. *J. Am. Chem. Soc.* **1975**, *97*, 3033-3038. (e) Ciliberto, E.; Doris, K. A.; Pietro, W. J.; Reisner, G. M.; Ellis, D. E.; Fragala, I.; Herbstein, F. H.; Ratner, M. A.; Marks, T. J. *J. Am. Chem. Soc.* **1984**, *106*, 7748-7761.

0002-7863/91/1513-1610$02.50/0

properties of these compounds have been extensively investigated in recent years. Single-crystal x-ray data show that the interplanar spacing of the Pc rings is approximately 3.32 Å, permitting significant through-space ($\pi-\pi$) interactions to occur.[7e] It is believed that these interactions are also present in solution, giving rise to the observed voltammetry.[6] An independent oxidation process is observed for each macrocycle in the oligomer. As the number of redox centers increases, the potential for the first oxidation process occurs at a less positive value and the potential difference between successive redox events becomes smaller.

Polymeric group 4a phthalocyanines have been synthesized and extensively characterized by a number of investigators for nearly 30 years.[10] These materials are simply the corresponding polymers (n = 25–120) of the silicon phthalocyanine oligomers described above. Marks and others have oxidized and reduced (doped) these polymers in the solid state by both chemical and electrochemical means, yielding highly conductive solids.[9a,10e,g,j-m] Electrochemical doping of the insoluble silicon polymers ($[Si(Pc)O]_n$, n = 120) as a slurry or microcompaction results in wide variations in the degree of partial oxidation or band filling (0.00–0.67).[10m] The percent oxidation vs potential doping profiles imply a smooth continuous process occurring over a 700–1100-mV range, depending on the counterion employed and the degree of oxidation obtained. Incremental doping with a variety of chemical oxidants results in materials with a degree of oxidation as high as 1.63.[10e,j-l] Regardless of the methodology, the oxidation of the polymer has been shown to be greatly influenced by structural changes accompanying the initial oxidation process.[10e,j-m]

Hanack and co-workers have reported synthetic and physicochemical data on soluble tetrasubstituted phthalocyaninato macromolecules $[M(R_4Pc)O]_n$, where M = Si and Ge and R = *tert*-butyl and TMS.[10d,h,i,11] These soluble analogues of the unsubstituted Pc polymers investigated by Marks were heterogeneously and homogeneously doped with halogens. The resulting materials exhibited conductivities that were 3–4 orders of magnitude higher than those of the neutral compounds.[10h] The relatively high solubility of these polymers in conventional solvents (~1.5 mg mL^{-1}) makes them ideal candidates for investigating the interactions between identical redox centers in large macromolecular assemblies by conventional electrochemical techniques.

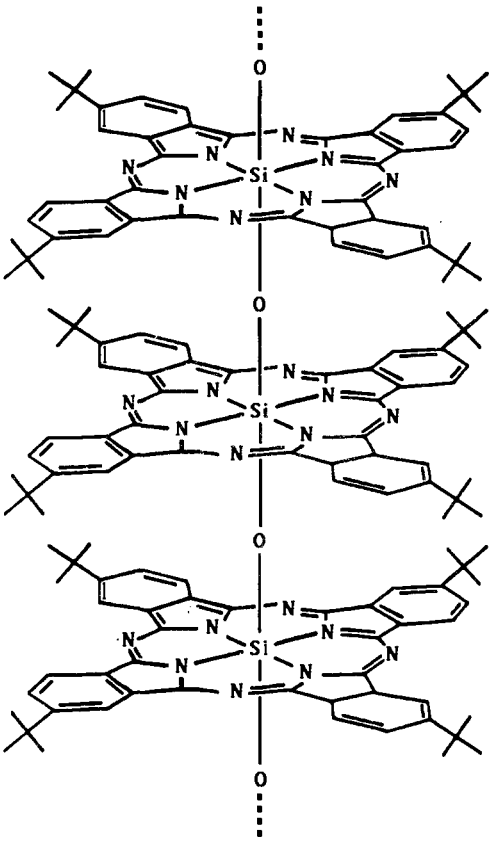

Figure 1. Schematic representation of the μ-oxo-(tetra-*tert*-butylphthalocyaninato)silicon polymer, $[Si[(t\text{-}Bu)_4Pc]O]_n$.

In this contribution, we report our electrochemical results for the oxidation of the tetra-*tert*-butyl substituted silicon polymer (μ-oxo-(tetra-*tert*-butylphthalocyaninato)silicon; Figure 1). Its voltammetry is compared and contrasted to that of the dicapped monomer (bis(trimethylsiloxy)(tetra-*tert*-butylphthalocyaninato)silicon). Digital simulations of the electrochemical results are used to model the system and estimate the amount of interaction between the redox centers. These results may prove germane to understanding the electrochemical properties of conventional redox polymers, chemically modified electrodes, biological systems, and electrically conductive materials.

Experimental Section

Solvents. Pyridine was dried and purified by distillation from CaH_2. Quinoline was purified and dried by vacuum distillation from CaH_2 after stirring over BaO. 1,1,2,2-Tetrachloroethane (98% Aldrich Chemical, Milwaukee, WI) was stirred over CaH_2 for 48 h and then vacuum distilled. The resulting solution was degassed on a high-vacuum line (10^{-5} Torr) by employing several freeze–pump–thaw cycles and then vacuum transferred to a greaseless specially designed round-bottom solvent bulb containing activated 3-Å molecular sieves. Reagent grade toluene, hexane, and anhydrous diethyl ether were used as received.

Reagents. Trimethylchlorosilane, capping reagent for the monomer, was obtained from Fluka (>98%, Fluka Chemie AG, Ronkonkoma, NY) and was used as received. $SiCl_4$ (99% Aldrich), employed in the synthesis of dichloro(tetra-*tert*-butylphthalocyaninato)silicon, was used without further purification. Tetrabutylammonium fluoroborate ($(TBA)BF_4$, electrometric grade, Southwestern Analytical Chemicals, Austin, TX), used as supporting electrolyte, was recrystallized from ethyl acetate/diethyl ether and dried under dynamic vacuum (10^{-5} Torr) for 2 days. Activated alumina (Grade I, 60–80 mesh), used in the purification of the capped monomer, was purchased from Fisher Scientific (Pittsburgh, PA) and was used as received. Deuterated chloroform (99.8%) was purchased from Cambridge Isotope Laboratories (Woburn, MA).

Electroactive Compounds. The μ-oxo-(tetra-*tert*-butylphthalocyaninato)silicon polymer was synthesized by employing a slight modification of the literature procedure.[10h,11] The dichloro(tetra-*tert*-butylphthalocyaninato)silicon precursor was prepared by reacting 5-*tert*-bu-

(8) (a) Mezza, T. M.; Armstrong, N. R.; Kenney, M. E. *J. Electroanal. Chem.* **1984**, *176*, 259–273. (b) Mezza, T. M.; Linkous, C. L.; Shepard, V. R.; Armstrong, N. R.; Nohr, R.; Kenney, M. E. *J. Electroanal. Chem.* **1981**, *124*, 311–320.

(9) (a) Skotheim, T. A., Ed. *Handbook of Conducting Polymers*; Dekker: New York, 1986; Vols. 1 and 2. (b) Ferraro, J. R.; Williams, J. M. *Introduction to Synthetic Electrical Conductors*; Academic Press: New York, 1987. (c) Skotheim, T. A., Ed. *Electroresponsive Molecular and Polymeric Systems*; Dekker: New York, 1988; Vol. 1. (d) Jerome, D., Caron, L. G., Eds. *Low-Dimensional Conductors and Superconductors*; Plenum: New York, 1987. (e) Proceedings of the International Conference on Science and Technology of Synthetic Metals (ICSM '88). *Synth. Met.* **1988–1989**, *27–29*. (f) Cowan, D. O.; Wiygul, F. M. *Chem. Eng. News* **1986**, *64(29)*, 28–45. (g) Ward, M. W. *Electroanalytical Chemistry*; Bard, A. J., Ed.; Dekker: New York, 1989; Vol. 16, pp 181–312. (h) Wudl, F. *Acc. Chem. Res.* **1984**, *17*, 227–232. (i) Scrosati, B. *Prog. Solid State Chem.* **1988**, *18*, 1–77.

(10) (a) Joyner, R. D.; Kenney, M. E. *J. Am. Chem. Soc.* **1960**, *82*, 5790–5791. (b) Joyner, R. D.; Kenney, M. E. *Inorg. Chem.* **1962**, *1*, 717–718. (c) Kroenke, W. J.; Sutton, L. E.; Joyner, R. D.; Kenney, M. E. *Inorg. Chem.* **1963**, *2*, 1064–1065. (d) Schneider, O.; Metz, J.; Hanack, M. *Mol. Cryst. Liq. Cryst.* **1982**, *81*, 273–284. (e) Dirk, C. W.; Inabe, T.; Schoch, K. F., Jr.; Marks, T. J. *J. Am. Chem. Soc.* **1983**, *105*, 1539–1550. (f) Diel, B. D.; Inabe, T.; Lyding, J. W.; Schoch, K. F., Jr.; Kannewurf, C. R.; Marks, T. J. *J. Am. Chem. Soc.* **1983**, *105*, 1551–1567. (g) Orthmann, E. A.; Enkelmann, V.; Wegner, G. *Makromol. Chem. Rapid Commun.* **1983**, *105*, 1551–1567. (h) Metz, J.; Pawlowski, G.; Hanack, M. *Z. Naturforsch.* **1983**, *38B*, 378–382. (i) Hanack, M.; Datz, A.; Fay, R.; Fishcher, K.; Keppeler, U.; Koch, J.; Metz, J.; Mezger, M.; Schneider, O.; Schulze, H. In *Handbook of Conducting Polymers*; Skotheim, T. A., Ed.; Dekker: New York, 1986; Vol. 1, and references therein. (j) Inabe, T.; Gaudiello, J. G.; Moguel, M. K.; Lyding, J. W.; Burton, R. L.; McCarthy, W. J.; Kannewurf, C. R.; Marks, T. J. *J. Am. Chem. Soc.* **1986**, *108*, 7595–7608. (k) Gaudiello, J. G.; Marcy, H. O.; McCarthy, W. J.; Moguel, M. K.; Kannewurf, C. R.; Marks, T. J. *Synth. Met.* **1986**, *15*, 115–128. (l) Moguel, M. K. Ph.D. Thesis, Northwestern University, Evanston, IL, 1986. (m) Gaudiello, J. G.; Kellogg, G. E.; Tetrick, S. M.; Marks, T. J. *J. Am. Chem. Soc.* **1989**, *111*, 5259–5271. (n) Almeida, M.; Gaudiello, J. G.; Kellogg, G. E.; Tetrick, S. M.; Marcy, H. O.; McCarthy, W. J.; Butler, J. C.; Kannewurf, C. R.; Marks, T. J. *J. Am. Chem. Soc.* **1989**, *111*, 5271–5284.

(11) For preparing the precursors to these polymers, see: Hanack, M.; Metz, J.; Pawlowski, G. *Chem. Ber.* **1982**, *115*, 2836–2853.

tyl-1,3-diiminoisoindoline[12] (5.0 g, 25 mmol) with $SiCl_4$ (4.1 mL, 36 mmol) in 42 mL of refluxing quinoline for 30 min under N_2. The resulting green solution, after being allowed to cool to room temperature, was diluted with 400 mL of concentrated HCl and heated to 50 °C for 1 h. The dark blue precipitate that formed (~3 g) was collected by suction filtration and washed with copious amounts of concentrated HCl followed by distilled water. The crude product was further purified by soxhlet extraction using diethyl ether. After several days of continuous extraction, the ether washes became clear and 1.5 g of approximately 98% pure (NMR) material was isolated by taking the ether solution to dryness. Conversion to the polymer via the dihydroxy(tetra-*tert*-butylphthalocyaninato)silicon was accomplished as reported previously.[10h] Spectroscopic properties of the polymer (UV/vis, FTIR) were identical with those reported in the literature.[10h]

The dicapped monomer, bis(trimethylsiloxy)(tetra-*tert*-butylphthalocyaninato)silicon, was synthesized and purified by following the procedures outlined in the literature for the preparation of biaxially substituted silicon phthalocyanines.[6a-c,7e] Trimethylchlorosilane (1.0 mL, 0.86 g, 7.9 mmol) was refluxed with dried $([t\text{-Bu}]_4\text{Pc})\text{Si(OH)}_2$ (100 mg, 0.13 mmol) in 20 mL of dry pyridine under N_2 for 5 h. The resulting solution was taken to dryness and the excess silane was removed in vacuo (10^{-3} Torr). The dried solids were chromatographed on alumina with toluene/hexane (1:2) as the eluant. The desired product was the first major band to elute. The isolated yield was 15%. Several weaker bands were also present and are believed to be higher weight oligomers.[6b,c,7e] Their limited concentration prevented characterization. The NMR and UV/vis spectra for the monomer are similar to those reported for other dicapped silicon phthalocyanines.[6a-c,7e] NMR data was obtained in $CDCl_3$ and had the following features: δ 9.55 (m, 3, 6-Pc), 8.39 (m, 5-Pc), 1.81 (s, *t*-Bu), -2.88 (s, CH_3). UV/vis data recorded in CH_2Cl_2 showed absorptions at 672*, 642, 605, 352*, and 336 nm. (The asterisk denotes major transitions.) Fast atom bombardment (FAB) mass spectral analysis from a 3-nitrobenzyl alcohol matrix showed two predominate peaks at *m/z* values of 942.6 and 1096. These peaks correspond to the dicapped monomer and monomer + 3-nitrobenzyl alcohol, respectively.

Instrumentation. Electrochemical measurements were performed with either a PAR Model 273 potentiostat/galvanostat (Princeton Applied Research, Princeton, NJ) or a BAS 100A electrochemical analyzer (Bioanalytical Systems Inc., West Lafayette, IN). Rotating disk voltammograms were obtained by using an AFMSR high-speed rotator in conjunction with a platinum disk electrode having a radius of 0.228 cm (Pine Instruments Grove City, PA). UV/vis spectroscopy was performed with a Beckman DU-64 spectrometer (Beckman Instruments, Fullerton, CA). Spectra were obtained with 1-cm matched quartz cells. Proton NMR spectra were acquired in the pulsed Fourier transform mode by using a Bruker (Billerica, MA) WM-250 250-MHz instrument. All the spectra are referenced to TMS (δ = 0.00). Fourier transform infrared spectra were obtained on either a Nicolet 5-DX or Nicolet 740 instrument (Nicolet Instruments, Madison, WI) as Nujol mulls using KBr plates. Mass spectra data was obtained by using a Finnigan TSQ-70B triple-stage quadrupole instrument operating in the Q1 MS mode and fast atom bombardment configuration (Finnigan Instruments, San Jose, CA). The instrument used a JEOL MS FAB atom source (JEOL Instruments, Boston, MA) operated at 20 °C, a filament current of 10 mA, and an acceleration voltage of 6 kV.

Electrochemical Cells and Procedures. Several types of electrochemical cells that interface directly to a high-vacuum line through ground-glass joints were used in these studies. Controlled-potential coulometry was carried out in an all-glass three-compartment cell.[13] The counter electrode, constructed of Pt gauze, was isolated from the working electrode compartment by two fine-porosity glass frits. The reference electrode, a Ag wire, was separated from the working cell compartment by a fine-porosity glass frit. The working electrode for bulk coulometry studies was constructed from Pt gauze and was approximately 8 cm^2 in area. A small-area (0.0180 cm^2) platinum disk working electrode (Bioanalytical Systems Inc.) was also placed in the working compartment of the cell to allow voltammetric studies to be performed. The small-area Pt working electrode was polished with 0.05-μm alumina (Buehler, Lake Bluff, IL) prior to use.

Experiments involving only diffusional voltammetric measurements (cyclic voltammetry, differential pulse voltammetry, chronocoulometry) were performed in single-compartment cells that also interfaced to a high-vacuum line through a ground-glass joint.[14] A small 0.0180-cm^2 area platinum disk working electrode, a platinum wire counter electrode, and a Ag wire reference electrode were used in these cells.

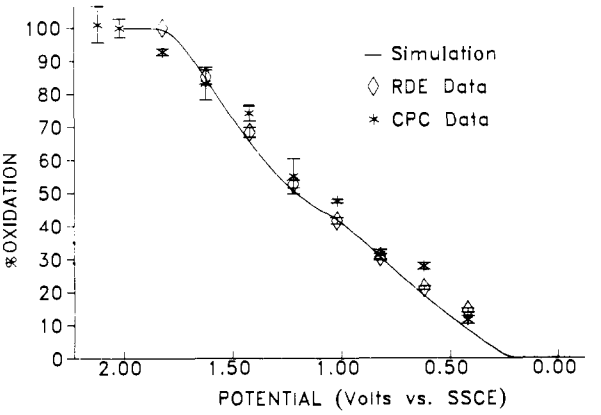

Figure 2. Degree of oxidation vs potential for the electrochemical oxidation of $[Si[(t\text{-Bu})_4Pc]O]_n$ in 1,1,2,2-tetrachloroethane/0.2 M $TBABF_4$. For the CPC data (*), each point corresponds to the mean value for a complete oxidation/reduction cycle. The error bars represent the difference between the oxidation and reduction values. Solutions were typically 20–40 μM (0.40–0.80 mg mL^{-1}). The percent oxidation values were determined by using eq 1. The mean RDE values (◊) were determined by averaging the current at different rotation rates by use of eq 4. The error bars represent the standard deviation. The solid line (—) represents the values calculated from the digital simulation.[29]

Rotating disk voltammetry experiments were performed in a three-compartment cell specially designed to reduce the formation of a vortex.[15] A Ag wire reference electrode and a Pt gauze counter electrode were placed in sidearm compartments separated from the main part of the cell by fine-porosity glass frits.

All solvents used in the electrochemical experiments were vacuum transferred directly into electrochemical cells containing a known amount of supporting electrolyte and the compounds of interest by using a high-vacuum (10^{-5} Torr) dual-manifold vacuum line. The concentration of supporting electrolyte was 0.2 M for all experiments. After solvent transfer, the electrochemical cells were back-filled with argon (Matheson, 99.95%) to ensure their anaerobic integrity. The argon was passed through a drying column (Mn on silica) to remove residual oxygen and moisture.

Digital Simulations. Digital simulations were performed utilizing the finite-differences method.[16] The polymer system was modeled as a material undergoing sequential reversible (Nernstian) electron transfer. The procedures employed for cyclic and rotating disk voltammetry are essentially identical with those used to model single-charge-transfer systems.[16a,c] The main difference between the models employed for these multicomponent systems and the others described in the literature are the equations used to describe the initial and surface boundary conditions and the dimensionless current. Differential pulse voltammograms were modeled as a series of potential-step experiments where the initial bulk concentration for each oxidation state of a species was set to a specific value depending on the base potential of the pulse.[17] A comprehensive description of these simulation techniques will be presented elsewhere.[18]

Results

Controlled-Potential Coulometry. Shown in Figure 2 is the percent oxidation as a function of potential for the silicon polymer determined from a series of controlled potential coulometry (CPC) experiments. Each point on the graph represents the percent oxidation determined by averaging the amount of charge passed for the initial oxidation of a solution of neutral polymer and the subsequent reduction back to the neutral compound at 0.00 V.

(12) The synthesis of the diiminoisoindoline involves several steps described in the following articles: (a) Larner, B. W.; Peters, A. T. *J. Chem. Soc.* **1952**, 680–686. (b) Mikhalenko, S. A.; Barkanova, S. V.; Lebedev, O. L.; Luk'yanets, E. A. *Zh. Obshch. Khim.* **1971**, *41*, 2735–2739. (c) Brach, P. J.; Grammatica, S. J.; Ossanna, O. A.; Weinberger, L. *J. Heterocycl. Chem.* **1970**, *7*, 1403–1405. (d) Reference 11.

(13) Smith, W. H.; Bard, A. J. *J. Am. Chem. Soc.* **1975**, *97*, 5203–5210.

(14) Tokel, N. E.; Keszthelyi, C. P.; Bard, A. J. *J. Am. Chem. Soc.* **1972**, *94*, 4872–4877.

(15) Puglisi, V. J.; Bard, A. J. *J. Electrochem. Soc.* **1972**, *119*, 829–833.

(16) (a) Feldberg, S. W. In *Electroanalytical Chemistry*; Bard, A. J., Ed.; Marcel Dekker: New York, 1969; Vol. 3, pp 199–296. (b) Prater, K. B.; Bard, A. J. *J. Electrochem. Soc.* **1970**, *117*, 207–213. (c) Britz, D. *Digital Simulations in Electrochemistry, Lecture Notes in Chemistry*; Springer-Verlag: Heidleberg, 1981. (d) Feldberg, S. W. In *Computers in Chemistry and Instrumentation*; Mattson, J. S., Mark, H. B., MacDonald, H. C., Eds.; Marcel Dekker: New York, 1972; Vol. 2, pp 185–215.

(17) Rifkin, S. C.; Evans, D. H. *Anal. Chem.* **1976**, *48*, 2174–2180.

(18) Chapaton, T. C.; Gaudiello, J. G., manuscript in preparation.

The error bars depict the difference between the two values.[19] The percent oxidation was determined by relating the amount of net charge passed at a specific potential to the mass of polymer present. Assuming that each phthalocyanine moiety (repeat unit) represents a one-electron redox site,[6] and given that its molecular formula is OSi[(*t*-Bu)$_4$Pc] ($C_{48}H_{48}N_8SiO$, gfw = 781.1), the degree of partial charge transfer is given by eq 1, where F is the Faraday

$$\% \text{ charge transfer} = \frac{\text{coulombs}}{(\text{grams of polymer/gfw of repeat unit})F} \times 100 \quad (1)$$

constant, 96 485 C mol^{-1}. A value of 100% represents the removal of one electron per phthalocyanine moiety. Note, this analysis does not assume any particular degree of polymerization, but simply relates the amount of charge passed to the number of moles of redox sites or repeat units.

The redox process for the oxidation of the polymer occurs over a 1750-mV range and represents the conversion between neutral material and the one-electron oxidation of each phthalocyanine site. This broad continuous fractional redox response is unlike the CPC behavior of conventional redox couples or polymers composed of noninteracting centers.[20] These materials undergo integral changes in their oxidation state over a narrow potential range, typically several hundred millivolts.[2,3] The observed response of the polymer is indicative of a material in which there is a large amount of interaction between the redox sites.[2,5] This is not surprising based on the solid-state properties of these systems.[10i]

The small difference in the amount of charge passed (±5%, within the experimental error of the technique) for an oxidation/reduction cycle and the continuous smooth redox profile suggest that no redox activity is gained or lost upon cycling. Isolation and spectroscopic characterization (UV/vis, FTIR) of the polymer, after cycling to all potentials set out in Figure 2, also indicate that the polymer is stable toward oxidation. The optical spectrum of the cycled material is identical with the neutral unoxidized material. The infrared spectrum exhibited the typical phthalocyanine bands, including the Si–O–Si asymmetrical stretch at 980 cm^{-1}.[10h,i] If the polymer was degrading into molecular species or small oligomers, the smooth, wide oxidation profile shown in Figure 2 would not be observed, even if no redox activity was lost.[21] Instead, a sharp change in the percent oxidation, similar to that observed for the CPC of a conventional redox couple, would be seen. In addition, oxidizing the polymer at 2.02 V (100% oxidation) and reducing back to neutral material results in a material with properties that are identical with those of the pristine polymer. Further proof of chemical stability was obtained from voltammetric measurements of the polymer after each CPC cycle. As discussed below in more detail, differential pulse voltammetry (DPV) can be employed to accurately characterize the redox behavior of these types of systems. The DPV response of the neutral cycled and pristine polymer are virtually identical, indicating again that the polymer is stable at all degrees of oxidation and simply undergoes a charge-transfer reaction at the electrode during the CPC experiments.

(19) These values are corrected for the constant background (residual) current, typically <1% of the initial current, measured at the given potential. The net coulombs at each potential were calculated by subtracting the product of the steady-state background current and the time of the experiment from the number of measured coulombs. As expected for a simple uncomplicated charge-transfer process, the current during the experiment decayed exponentially with time.[20]

(20) (a) Bard, A. J.; Faulkner, L. R. *Electrochemical Methods*; Wiley, New York, 1980. (b) Bard, A. J.; Santhanam, K. S. V. In *Electroanalytical Chemistry*; Bard, A. J., Ed.; Marcel Dekker: New York, 1970; Vol. 4, pp 215–315.

(21) Electrochemical reduction of the corresponding germanium polymer shows a similar broad continuous redox response from 0 to 100% reduction. At potentials more negative than those required to obtain 100% reduction, the polymer degrades into monomeric units, which are still electroactive. Even though no redox activity is lost, the same number of coulombs are passed for oxidation of the reduced material back to the neutral form as were passed during the initial reduction; the percent reduction vs potential profile is like that observed for a conventional redox couple and not the broad response observed initially.

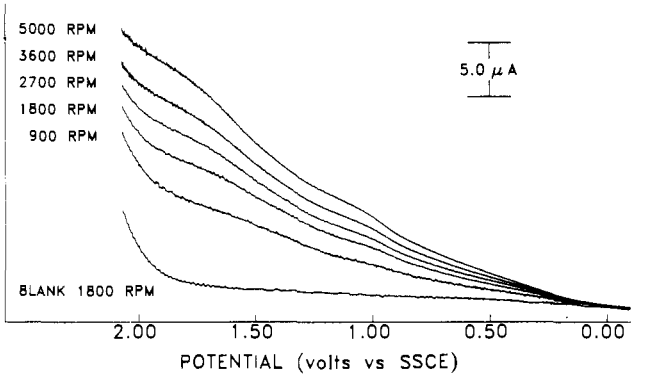

Figure 3. Rotating disk electrode voltammograms for the oxidation of 32.1 μM (0.627 mg mL^{-1}) solution of {Si[(*t*-Bu)$_4$Pc]O}$_n$ in 1,1,2,2-tetrachloroethane/0.2 M TBABF$_4$ at a 0.228-cm^2 Pt electrode. The increase in current at 1.80 V is due to the oxidation of the solvent.

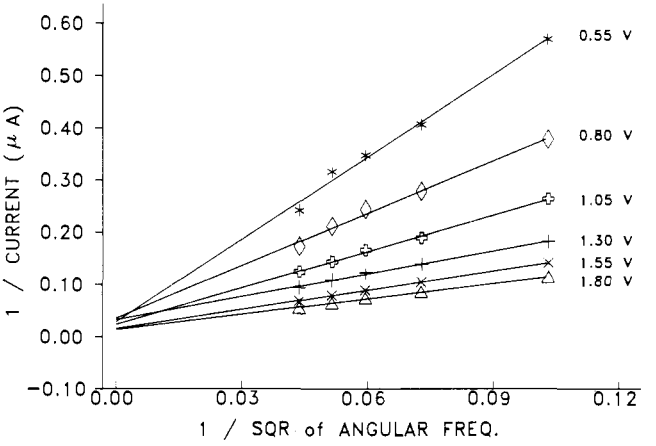

Figure 4. Plot of (disk current)$^{-1}$ at various potentials and rotation rates vs $\omega^{-1/2}$ for the oxidation of {Si[(*t*-Bu)$_4$Pc]O}$_n$ in 1,1,2,2-tetrachloroethane/0.2 M TBABF$_4$. The linear behavior is indicative of Nernstian behavior.

Rotating Disk Voltammetry. Conventional voltammetry was also used to characterize the redox properties of this material. Shown in Figure 3 are a series of rotating disk electrode (RDE) voltammograms obtained at different rotation rates for the oxidation of the polymer and the background current observed for a blank solution. The oxidation process for the polymer again occurs over a broad potential range (~1750 mV) and reaches a limiting current near 1.80 V. The increase in current near 1.85 V is a background process arising from the oxidation of the solvent. For comparison, a RDE voltammogram of a conventional one-electron redox couple exhibits a response over only a 200-mV potential region.[22] The shapes of the voltammograms are independent of angular frequency ($\omega = 2\pi f$, where f is the rotation rate) and increase in magnitude with $\omega^{1/2}$ at all potentials. A plot of (current)$^{-1}$ vs $\omega^{-1/2}$ (Figure 4) yields straight lines that intersect near the origin. This behavior is expected only for totally reversible (Nernstian) systems and suggests that there are no kinetic limitations for the oxidation of the polymer anywhere along the entire voltammogram.[22]

The limiting current near 1.82 V suggests that the polymer has reached its maximum degree of oxidation. This correlates with the CPC data (Figure 2), which also reach a limiting value near 1.80 V. If the limiting current in the voltammogram arises from some known degree of oxidation and the concentration of the polymer is known, a diffusion coefficient for the polymer can be calculated from the Levich equation:[22]

$$i_l = 0.62 n_p F A C^*_p D_p^{2/3} \nu^{-1/6} \omega^{1/2} \quad (2)$$

(22) (a) Levich, V. G. *Physicochemical Hydrodynamics*; Prentice-Hall: Englewood Cliffs, NJ, 1962. (b) Reference 20a.

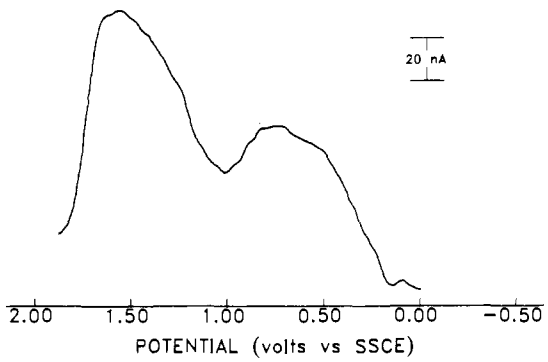

Figure 5. Differential pulse voltammogram for the oxidation of a 64.0 μM (1.25 mg mL^{-1}) solution of $\{Si[(t\text{-}Bu)_4Pc]O\}_n$ in 1,1,2,2-tetrachloroethane/0.2 M $TBABF_4$ at a 0.0180-cm^2 Pt electrode. Pulse amplitude 50 mV, pulse width 50 mS, pulse period 1000 mS, scan increment 4 mV s^{-1}.

where i_l is the limiting current, n_p is the number of electrons associated with the oxidation of the polymer, A is the area of the electrode, C^*_p is the bulk concentration of the polymer, D_p is the diffusion coefficient of the polymer, ν is the kinematic viscosity of the solvent (0.0120 cm^2 s^{-1} for 1,1,2,2-tetrachloroethane[23]), and the other terms are as defined above. On the basis of an end-group tritium-labeling study, Hanack and co-workers estimated the degree of polymerization of the polymer to be ~25.[10i,24] With this value the concentration of the polymer solution can be calculated. Assuming that each phthalocyanine ring in the polymer undergoes a one-electron oxidation (as suggested by the CPC data), a diffusion coefficient of (2.5 ± 0.3) × 10^{-7} cm^2 s^{-1} is calculated.[22] Background-corrected chronocoulometry data obtained at 1.90 V give similar results. This value is similar to the diffusion coefficient of other electroactive polymers of comparable molecular weight and, as discussed below, correlates well with the diffusion coefficient of the dicapped monomer and other silicon phthalocyanine systems.[2,3c]

The percent oxidation vs potential curve can also be calculated from the RDE voltammograms. The current at any potential for a RDE voltammogram is given by

$$i = 0.62nFAC^*D^{2/3}\nu^{-1/6}\omega^{1/2}[C^* - C(y=0)] \qquad (3)$$

where $C(y = 0)$ is the concentration of the initial (unoxidized) form of the electroactive material at the electrode surface.[22] Dividing eq 3 by the Levich equation (eq 2) yields

$$\frac{i}{i_l} = \frac{[C^{*o} - C(y=0)]}{C^*} = \text{fraction of material that has undergone electron transfer} \qquad (4)$$

Assuming that the limiting current corresponds to 100% oxidation (as suggested by the CPC results), the percent oxidation vs potential curve can be calculated by dividing the current at any potential by the limiting current. These data are shown in Figure 2. There is good agreement between the CPC and RDE experiments, two inherently different techniques for determining the percent oxidation. This correlation is additional proof that the voltammograms represent the Nernstian oxidation of the polymer. The RDE experiments effectively "map out" the thermodynamic potentials for the entire oxidation process of the polymer. The voltammograms also indicate that the oxidation process is relatively continuous over the entire potential range and that there is no large degree of stability at any particular degree of oxidation. A sharp increase in the current at a specific potential would be expected if this was the case.

Differential Pulse Voltammetry. The rather featureless response for the percent oxidation vs potential profile obtained from the CPC and RDE experiments led to the use of differential pulse voltammetry to more accurately probe the energetics (potential dependence) of the oxidation process. The derivative output of DPV makes it extremely sensitive to subtle changes in redox chemistry and an ideal technique for the characterization of multicomponent systems.[25] A DPV is essentially a derivative of a RDE voltammogram. Shown in Figure 5 is the DPV for the oxidation of the silicon polymer. The current response shows that the oxidation is not a smooth continuous process over the entire potential range. The voltammogram appears to contain two distinct regions of electroactivity. The potential range of electroactivity is similar to that observed in the CPC and RDE experiments. As expected, the potential for the decrease in current at 1.85 V correlates with the potential for the limiting current observed in the RDE voltammograms. The current response for both techniques at those potentials arises from 100% oxidation of the polymer.

On the basis of the RDE data (rapid kinetics), it is believed that the shape of the DPV results from the Nernstian oxidation of the polymer. Since the pulse sequence employed for DPV effectively performs a preelectrolysis of the electroactive species near the surface of the electrode before the current is measured, the voltammogram illustrates the ease with which the polymer goes from one fractional oxidation state to another. The break near 1.0 V may imply that there is some inherent stability for that fractional degree of oxidation (~50%). It is clear from the DPV response that the polymer does not undergo a constant incremental change in oxidation state with potential. Furthermore, the smooth profile also suggests that the material under study does not contain an appreciable (detectable) amount of smaller length oligomers. The redox response of these compounds would occur over a several hundred millivolt range, exhibiting a sharp increase in current at specific potentials. Such behavior has been observed for numerous types of cofacially jointed silicon phthalocyanine systems, including the monomer as discussed below, by using various electrochemical techniques.[6]

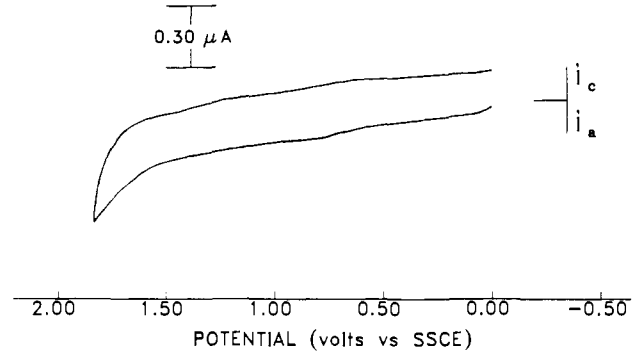

Figure 6. Cyclic voltammogram for the oxidation of a 64.0 μM (1.25 mg mL^{-1}) solution of $\{Si[(t\text{-}Bu)_4Pc]O\}_n$ in 1,1,2,2-tetrachloroethane/0.2 M $TBABF_4$ at a 0.0180-cm^2 Pt electrode. Scan rate 100 mV s^{-1}.

Cyclic Voltammetry. Shown in Figure 6 is a cyclic voltammogram for the oxidation of a 64.0 μM solution of the polymer (1.08 mg mL^{-1}). The potential is scanned over the same range as the DPV and RDE voltammograms reported earlier. The characteristic anodic and cathodic waves that are usually seen in the cyclic voltammograms of redox active systems, including polymers composed of noninteracting sites, are absent.[1a,2-4] The current–potential response is similar to the featureless capacitive charging current observed for a blank solution containing only supporting electrolyte. The current magnitude, however, is approximately 1 order of magnitude greater than that observed for a blank solution. The increase in current near 1.85 V is again assigned to the oxidation of the solvent. The shape of the wave is invariant with changes in scan rate (v) and the current varies with $v^{1/2}$. The properties of the CV are characteristic of a Nernstian oxidation to form a chemically stable product.[26] The

(23) Riddick, J. A.; Bunger, W. B.; Sakano, T. K. *Organic Solvents; Physical Properties and Methods of Purification*; Wiley-Interscience: New York, 1986; p 522.
(24) Marks, T. J., private communication.
(25) Parry, E. P.; Osteryoung, R. A. *Anal. Chem.* **1965**, *37*, 1634–1637.
(26) Nicholson, R. S.; Shain, I. *Anal. Chem.* **1964**, *36*, 706–723.

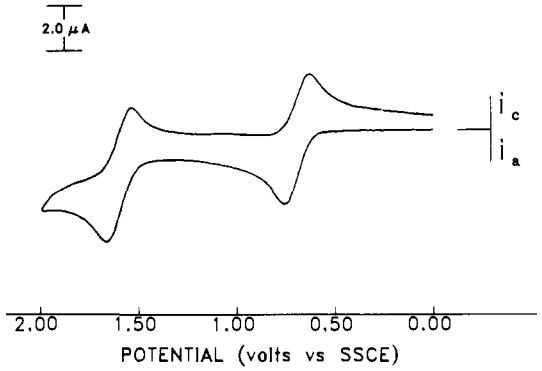

Figure 7. Cyclic voltammogram for the oxidation of a 1.08 μM (1.02 mg mL^{-1}) solution of $(CH_3)_3SiOSi[(t\text{-}Bu)_4Pc]OSi(CH_3)_3$ in 1,1,2,2-tetrachloroethane/0.2 M $TBABF_4$ at a 0.0180-cm^2 Pt electrode. Scan rate 100 mV s^{-1}.

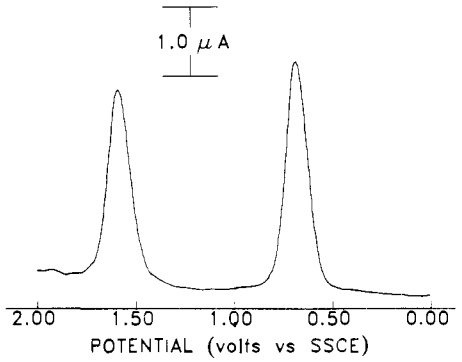

Figure 8. Differential pulse voltammogram for the oxidation of a 1.08 μM (1.02 mg mL^{-1}) solution of $(CH_3)_3SiOSi[(t\text{-}Bu)_4Pc]OSi(CH_3)_3$ in 1,1,2,2-tetrachloroethane/0.2 M $TBABF_4$ at a 0.0180-cm^2 Pt electrode. Pulse amplitude 50 mV, pulse width 50 mS, pulse period 1000 mS, scan increment 4 mV s^{-1}.

voltammogram also exhibits a slight decrease in current near 1.0 V both for the initial oxidation and subsequent reduction. This correlates well with the change in slope observed in the RDE voltammograms and the dip seen in the DPV near that potential. As described below, via digital simulations of the electrochemical responses, the polymer can be modeled as a series of reversible redox couples in equilibrium with one another. This gives rise to a CV response that is nearly identical with that shown in Figure 6.

Electrochemical Characterization of Bis(trimethylsiloxy)(tetra-*tert*-butylphthalocyaninato)silicon. To aid in understanding the complex nature of the polymer voltammetry, the redox chemistry of the bis(trimethylsiloxy)(tetra-*tert*-butylphthalocyaninato)silicon, the trimethylsilyl dicapped monomer, was investigated under identical conditions. The electrochemical characterization of numerous types of monomeric silicon phthalocyanines has been extensively studied in recent years.[6] All of these materials undergo a single Nernstian one-electron oxidation to form a stable cation radical. Shown in Figures 7 and 8 are the CV and DPV for a 1.08 μM solution of the monomer in $C_2H_2Cl_4$ scanned over the same potential range as the polymer (Figures 5 and 6). The CV exhibits two reversible oxidation waves at $E_{1/2}$ = 0.66 V and $E_{1/2}$ = 1.56 V, which are characteristic of one-electron Nernstian processes.[26] The $i_{pa}/v^{1/2}C$ (i_{pa} is the anodic peak current) values are constant with scan rate, i_{pa}/i_{pc} (i_{pc} is the cathodic peak current) are near unity, and the peak separation for each wave ($E_{pa} - E_{pc}$) is approximately 60 mV. The E_{pa} value for each wave is also invariant with scan rate.

The DPV of the same solution also shows two responses characteristic of successive Nernstian one-electron oxidations to form stable products. The widths at half-height of both peaks are approximately 100 mV ($W_{1/2}$ = 3.52 RT/nF, or 90.4 mV for a one-electron reversible processes at 25 °C).[25] The CV and DPV results both suggest that the monomeric material undergoes two one-electron oxidations to form stable mono- and dications. While most biaxially substituted silicon phthalocyanine monomers exhibit a one-electron oxidation per Pc ring, the 2+ oxidation state for each site is less often obtained. The silicon naphthalocyanine compound undergoes two one-electron oxidations to form a stable dication.[6b] The observation of the second oxidation wave in Figures 7 and 8 can be attributed to an inductive (electron donating) effect of the *tert*-butyl groups on the Pc ring.

The slight (15%) decrease in current for the second oxidation wave in Figure 8 is probably due to a smaller diffusion coefficient for the cation compared to the neutral compound. The diffusion coefficient of the neutral monomer was calculated from DPV, CV, and chronocoulometry data. The value was determined to be (3.0 ± 0.3) × 10^{-6} cm^2 s^{-1}. This value is similar to those found by Bard, Kenney, and co-workers for similar monomeric phthalocyanine species.[6b]

The relationship between molecular weight (M) and diffusion coefficient (D) for macromolecules has been well established from both a theoretical and experimental viewpoint. For randomly coiled polymers treated as spheres, the diffusion coefficient is predicted to vary as (molecular weight)$^{-0.55}$ in well-behaved solvents.[27] Good agreement has been observed by Bard, Funt, and others for numerous electroactive polymers (poly(vinylferrocene), poly(vinylnaphthalene), poly(vinylanthracene), and numerous anthraquinone polymers) in a wide variety of aprotic solvents.[2,3,28] For thin rodlike-shaped macromolecules with a constant diameter and a molecular length directly proportional to molecular weight, D has been predicted to vary as $M^{-0.81}$.[27] Electrochemical, UV/vis, and NMR studies of short-length oligomeric silicon phthalocyanines (n = 1–4) indicate significant interactions between the Pc rings, suggesting that these types of materials maintain their cofacial arrangement in solution.[6,7a-d] Assuming that the tetra-*tert*-butyl silicon polymer also maintains a cofacial, rodlike structure in solution, the relationship between diffusion coefficient and molecular weight of the polymer and monomer is give by eq 5, where D_m, M_m, D_p, and M_p are the

$$D_p = D_m(M_m/M_p)^{0.81} \quad (5)$$

diffusion coefficient and molecular weight of the dicapped monomer and polymer, respectively. Using eq 5, the diffusion coefficients determined from the electrochemical measurements reported earlier, and M_m (943.4 g mol^{-1}, $C_{54}H_{66}N_8Si_3O_2$) yields a value of (2.0 ± 0.4) × 10^4 g mol^{-1} for M_p. Letting M_p equal the product of the degree of polymerization of the polymer and the gfw of the repeat unit (781.1 gfw, $OSi[(t\text{-}Bu)_4Pc]$), a degree of polymerization of 26 ± 3 is calculated. This value shows close agreement with the value of 25 reported by Hanack, which was employed in the voltammetric analysis.[10i]

It is of interest to compare the magnitude of the electrochemical responses from solutions of the monomer and polymer obtained under the same conditions. The solutions used to obtain the CV and DPV of the monomer (Figures 6 and 7) and polymer (Figures 5 and 8) have the same concentration of *electroactive sites*. The concentration of the polymer solution is 25 times less than the monomer solution since the degree of polymerization is assumed to be 25. The average current is approximately 15 times smaller for the polymer than for the monomer as measured by both techniques. Although a factor of 3.5 can be ascribed to the difference in diffusion coefficients between the species ($D_m^{1/2}/D_p^{1/2}$, the current for each technique is proportional to $D^{1/2}$), the major reason for the decrease in current is that the redox response for the polymer is distributed over a much wider potential range than the monomer. The one-electron oxidation of the monomer occurs over a 200-mV range, the same degree of oxidation for the polymer occurs over 1750 mV.

Digital Simulations of the Voltammograms. To gain additional insight into the redox chemistry of the polymer, digital simulations

(27) Tanford, C. *The Physical Chemistry of Macromolecules*; Wiley: New York, 1961; p 362.
(28) Margerum, L. D.; Meyer, T. J.; Murray, R. W. *J. Phys. Chem.* **1986**, *90*, 2696–2702.

of the electrochemical responses were undertaken. These types of numerical methods have proven invaluable in elucidating the mechanism of complicated redox events.[16] On the basis of the CPC and RDE data (Nernstian electron transfer, one electron removed per Pc site at 100% oxidation), the polymer was modeled as an array comprised of redox couples that can undergo a one-electron reversible oxidation. Each center has its own unique standard potential (E^0) and is in equilibrium with the other sites of the assembly. The sequential Nernstian oxidation of the polymer can be represented as

$$R_n \rightleftarrows R_{n-1}O_1 + e^- \qquad E^0_1 \tag{6}$$

$$R_{n-1}O_1 \rightleftarrows R_{n-2}O_2 + e^- \qquad E^0_2 \tag{7}$$

$$\vdots$$

$$R_{n-(n-1)}O_{n-1} \rightleftarrows O_n + e^- \qquad E^0_n \tag{8}$$

where R represents neutral sites, O represents oxidized sites, and n represents the degree of polymerization, again taken as 25. Initially, the solution contains only species R_n (neutral polymer), all other oxidation states of the array are assumed absent. Since each couple of the polymer is in equilibrium with the electrode, their concentration is governed by the Nernst equation. The concentration of each species at the electrode surface at a given potential can be calculated from the potential-dependent equilibrium constant (K) describing each redox couple.

$$K_1 = \frac{[R_{n-1}O_1]_{x=0}}{[R_n]_{x=0}} = \exp(E - E^0_1)\frac{n_1F}{RT} \tag{9}$$

$$K_2 = \frac{[R_{n-2}O_2]_{x=0}}{[R_{n-1}O_1]_{x=0}} = \exp(E - E^0_2)\frac{n_2F}{RT} \tag{10}$$

$$\vdots$$

$$K_n = \frac{[O_n]_{x=0}}{[R_{n-(n-1)}O_{n-1}]_{x=0}} = \exp(E - E^0_n)\frac{n_nF}{RT} \tag{11}$$

where E is the applied electrode potential. For a polymer containing n redox sites, there are n redox couples and equilibrium expressions describing the distribution of $n + 1$ possible redox states. Mass balance requires that the sum of the concentrations of the individual species equals the initial neutral bulk concentration of the polymer $[R^*_n]$.

$$[R^*_n] = [R_n]_{x=0} + [R_{n-1}O_1]_{x=0} + [R_{n-2}O_2]_{x=0} + \ldots + [O_n]_{x=0} \tag{12}$$

Substituting the above equilibrium expressions in eq 12 yields

$$[R^*_n] = [R_n]_{x=0}[1 + K_1 + K_1K_2 + \ldots + K_1K_2K_3 \ldots K_n] \tag{13}$$

Dividing eq 13 into each of the equilibrium expressions above and rearranging results in a series of expressions for the normalized (fractional) concentration of each species with respect to the initial bulk concentration

$$\frac{[R_n]_{x=0}}{[R^*_n]} = \frac{1}{1 + K_1 + K_1K_2 + \ldots + K_1K_2 \ldots K_n} \tag{14}$$

$$\frac{[R_{n-1}O_1]_{x=0}}{[R^*_n]} = \frac{K_1}{1 + K_1 + K_1K_2 + \ldots + K_1K_2 \ldots K_n} \tag{15}$$

$$\vdots$$

$$\frac{[O_n]_{x=0}}{[R^*_n]} = \frac{K_1K_2 \ldots K_n}{1 + K_1 + K_1K_2 + \ldots + K_1K_2 \ldots K_n} \tag{16}$$

Knowing these surface boundary conditions and assuming a mode of mass transport for material to the electrode surface (diffusion for CV and DPV, diffusion and convection for RDE voltammetry) allows the simulation of any electrochemical technique involving a chemically stable system. These general procedures were employed to simulate the voltammetric responses of the silicon polymer.

Shown in Figure 9 are a series of simulated RDE voltammograms for a polymer containing 25 one-electron reversible redox couples in equilibrium with one another. The standard potentials used to generate the voltammograms were carefully chosen to produce a response similar to that observed for the silicon polymer. The values used are represented as vertical bars on the potential axis of Figure 9. The parameters used in the simulations for the area of the electrode, diffusion coefficient, concentration, kinematic viscosity, and angular frequency are the same as those used in the analysis of the experimental data. The simulated voltammograms show good agreement with the experimental results (Figure 3) for all rotation rates. The magnitudes of limiting currents reached near 1.80 V are nearly the same as those observed experimentally (minus the background processes). The percent oxidation vs potential profile calculated from the simulation closely matches the experimental CPC and RDE results.[29] These values are compared in Figure 2.

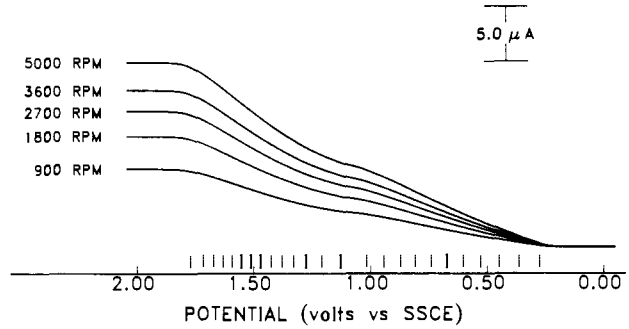

Figure 9. Simulated rotating disk voltammograms for the oxidation of $\{Si[(t\text{-}Bu)_4Pc]O\}_n$. The standard potentials used to model the system are represented by vertical lines on the potential axis. The simulation conditions were the same as those of the experimental data, Figure 2 (n_p = 25, A = 0.228 cm^2, C^*_p = 32.1 μM, D_p = 2.47 × 10^{-7} cm^2 s^{-1}, n = 0.0120 cm s^{-1}).

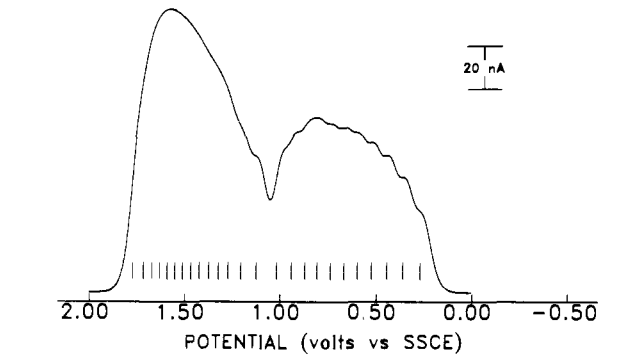

Figure 10. Simulated differential pulse voltammogram for the oxidation of $\{Si[(t\text{-}Bu)_4Pc]O\}_n$. The standard potentials used to model the system are represented by vertical lines on the potential axis. The simulation conditions were the same as those in the experimental data, Figure 4 (n_p = 25, A = 0.0180 cm^2, C^*_p = 64.0 μM, D_p = 2.47 × 10^{-7} cm^2 s^{-1}, pulse amplitude 50 mV, pulse width 50 mS, pulse period 1000 mS, scan increment 4 mV s^{-1}).

If the model used to simulate the RDE voltammograms accurately represents the redox chemistry of the system, the parameters used to describe the system should generate the correct response regardless of the technique. Shown in Figure 10 is a simulated DPV of the polymer employing the same diffusion coefficient and standard potentials used in the RDE simulations.

(29) The percent oxidation (or reduction) of an assembly comprised of multiple redox sites can be calculated by summing the weighted fractional concentrations of the different redox states.

$$\% \text{ oxidation} = \sum_{j=1}^{j=m} \frac{[R_{m-j}O]}{[R_m{}^*]} \sum_{k=1}^{k=j} n_k \times 100$$

where $[R_m{}^*]$ is the initial concentration of the assembly comprising m redox sites. $[R_{m-j}O_j]$ is the concentration of the species resulting from j sequential redox steps. n_k the total number of electrons involved in j sequential redox steps.

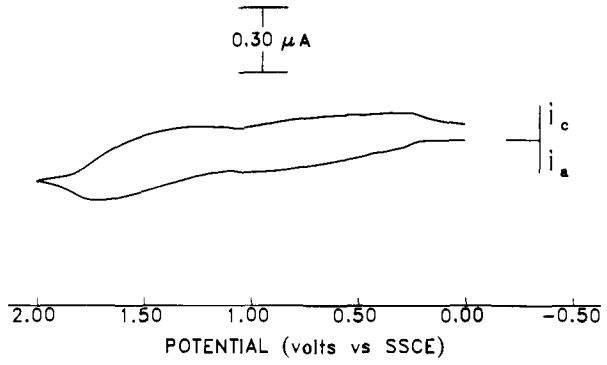

Figure 11. Simulated cyclic voltammogram for the oxidation of $[Si[(t\text{-}Bu)_4Pc]O]_n$. The standard potentials used to model the system were the same as those used for the RDE and DPV simulations. The simulation conditions were the same as those of the experimental data, Figure 6 (n_p = 25, A = 0.0180 cm^2, C^*_p = 64.0 μM, D_p = 2.47 × 10^{-7} cm^2 s^{-1}, scan rate 4 mV s^{-1}).

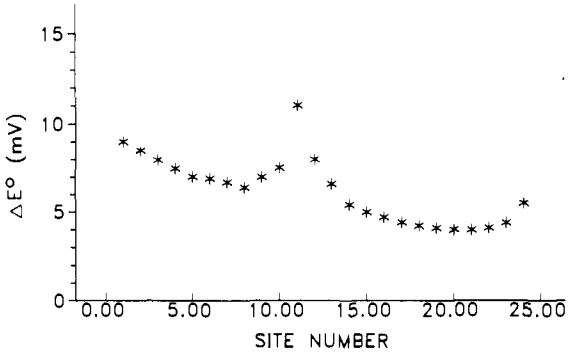

Figure 12. Difference in potential between successive standard potential values (E^0) used to simulate the voltammetric responses of the silicon polymer.

The polymer concentration, electrode area, and pulse amplitude and duration were set to match those used to obtain the experimental DPV shown in Figure 5. The agreement between the simulated and experimental voltammograms suggests that the model employed does represent the oxidation of the polymer. The nearly identical response is encouraging considering the high resolution of the technique in distinguishing closely spaced redox events. Small changes (±0.5 mV) in the standard potential values employed in the model caused significant changes in the shape of the simulated current response. The two distinct regions observed in the experimental DPV are also seen in the simulation. The break in current occurs at nearly the same potential and is approximately the same size as that observed in the experimental voltammograms.

The cyclic voltammetry response for the polymer was also simulated (Figure 11). Again, the same diffusion coefficients and standard potentials used in the other simulations were employed along with the experimental conditions corresponding to the experimental CV. The smooth featureless response is nearly identical with the experimental results in Figure 6. There is an almost constant current observed between 0.25 and 1.80 V. Similar behavior is observed experimentally. These results imply that the current observed for the polymer is indeed faradaic in nature and that the featureless CV is the correct response for a material comprised of multiple interactive sites.

Discussion

The broad uncharacteristic shape of the RDE voltammograms, CV, and DPV of the silicon polymer described above can result from a variety of factors. Effects arising from adsorption, precipitation, chemical instability of the reactants or products, structural changes accompanying the redox event, slow electron transfer, or interactions between the centers can give rise to the observed response.[1] The RDE voltammograms suggest no adsorption or precipitation before or after the oxidation process. As expected, the current at all potentials is a steady-state value and the voltrammograms have the same profile regardless of the direction of the potential scan. They exhibit no appreciable hysteresis upon potential reversal anywhere along the response and the limiting current increases as $\omega^{1/2}$, implying that the response is solely mass-transport limited at all rotation rates and potentials. The CPC and DPV results indicate that the polymer is chemically stable at all degrees of oxidation.

Analysis of the RDE data (Figure 4) also suggests that there is no detectable barrier to electron transfer for obtaining any degree of partial oxidation. The small nonzero intercept in the i^{-1} vs $\omega^{1/2}$ plot at earlier potentials (values ≤0.55 V) is probably due to a small amount of background current being included in these small current values (those ≤15% of the limiting current). This gives rise to a slight constant offset and the nonzero intercept. The agreement between the simulated voltammograms and the experimental results also implies that there is no kinetic barrier to oxidation; the simulation model is based solely on reversible redox couples.

Although the polymer exhibits reversible behavior at all potential and rotation rates, a lower limit for the heterogeneous electron-transfer rate constant (k_f) can be estimated from the RDE results.[22] Assuming a 10% change in the shape of the voltammograms could be detected, a lower limit for k_f can be approximated by[30]

$$k_f \cong 9D_p/\delta_o \qquad (17)$$

where $\delta_o \doteq 1.61\ D_p^{1/3}\omega^{-1/2}\nu^{1/6}$. Equation 17 estimates the conditions for the transition between a completely mass transport limited process to one being influenced by the charge-transfer event. With the values reported earlier for n, D_p, and the fastest rotation rate (5000 RPM) eq 17 yields a lower limit for k_f of 1 × 10^{-2} cm s^{-1} at any potential along the voltammogram. This value suggests that charge can be quickly shuttled between the polymer and an electrode at any potential. For comparison, the lower limit for the standard heterogeneous rate constants (k_s) for the oxidation of the dicapped unsubstituted monomer, dimer, and trimer [t-BuMe$_2$SiO(SiPcO)$_n$SiMe$_2$$t$-Bu, n = 1–3] was estimated by Armstrong et al. to be 3 × 10^{-3} cm s^{-1} in dichloromethane.[6a]

The unusual voltammetric behavior for the polymer appears to be due to the significant amount of through-space π orbital overlap between the phthalocyanine macrocycles composing the assembly.[7e,10c-o] In the absence of this interaction, the shape of the current–potential response would be identical with that of the first wave of the monomer and the standard potential for both systems would be the same.[2] The magnitude of the current for the polymer would, however, be dependent on the total number of redox sites. The onset of oxidation for the polymer at potentials 400 mV less positive than that of the monomer is due to the stability arising from the delocalization of charge among the redox centers comprising the polymer. When the difference between the standard potentials for a reversible system undergoing sequential electron transfer is less than approximately 100 mV, the current–potential curve is predicted to merge into a single broad multiple-electron response.[31] The digital simulation results can be used to estimate the difference in energy between each successive redox event and act as a guide to the amount of interaction between the centers. The nearly identical shape and magnitude between the experimental and simulated voltammograms and their agreement with the CPC data suggest that the E^0 values employed in the simulation can be used to represent the redox potentials of the polymer. Shown in Figure 12 are the potential differences between successive E^0 values used to model the polymer. The differences in standard potential between successive sites range from about 4 to 10 mV and appear to be grouped into two distinct regions. The potential difference for the first 10 sites (40% of the total number) averages 7.5 ± 0.8 mV while the difference

(30) Reference 20a, Chapter 8.
(31) Polcyn, D. S.; Shain, I. *Anal. Chem.* **1966**, *38*, 370–375. (b) Ammar, F.; Saveant, J. M. *J. Electroanal. Chem.* **1973**, *47*, 215–221, and references therein.

between the last 13 (52% of the total number) averages 5.0 ± 1.1 mV. It appears that the amount of interaction, as measured by these differences in standard potentials, is not constant over the entire range of oxidation states. A noticeable change occurs near the 50% value, corresponding to the dip in the voltammograms, and may indicate a change in how charge is distributed between the sites after the polymer has been oxidized 50%.

As mentioned earlier, various molecular and polymeric porphyrins and phthalocyanines are electrically conductive in the solid state when doped.[10c-o] Optical, magnetic, and PES measurements have been used to estimate the bandwidth of these conductors.[7e,10f,j,l,n,o] Most fall within the range of 0.5–0.7 eV and have been shown to be dependent on the nature of the counterions and the structure of the material. Any correlation between the homogeneous electrochemical results reported here and solid-state measurements depends on whether the redox site interactions occurring in solution for the soluble polymer are great enough to result in the formation of a band-type electronic structure. Spectroscopic measurements on various types of soluble conducting organic polymers indicate that they maintain their bandlike structure in solution.[32] Assuming similar behavior for the silicon polymer and having the ability to oxidize the material from 0 to 100% at Nernstian potentials suggest that the potential range for the oxidation process could be used to estimate the bandwidth of the polymer. The electrochemical results (CPC, DPV, RDE) effectively measure the thermodynamic energy range of redox states composing the polymer. This "redox-derived bandwidth" is approximately 3 times larger than the bandwidth of the unsubstituted polymer determined by conventional means in the solid state (1.75 V vs 0.6 eV). This would imply that a rigid band model alone is not applicable for modeling the electrochemical behavior of these systems.[33] The difference may be due to a change in the energy of the states as charge is removed from the polymer (i.e., the energy of the band shifts with the degree of oxidation or cumulative charging). This could account for the difference in the potential increments between the standard potentials observed in the two regions of the voltammograms discussed earlier. Any correlation between band structure and redox potentials must await a detailed spectroscopic characterization of the oxidized polymer in solution and electronic structure calculations as a function of oxidation level.[33]

(32) (a) Eisenbaumer, R. L.; Jen, K. Y.; Ododi, R. *Synth. Met.* **1986**, *15*, 169–174. (b) Patil, A. O.; Ikenoue, Y.; Wudl, F.; Heeger, A. J. *J. Am. Chem. Soc.* **1987**, *109*, 1858–1859. (c) Patil, A. O.; Ikenoue, Y.; Wudl, F.; Heeger, A. J. *Synth. Met.* **1987**, *20*, 151–159.

(33) Calculated bandwidth and structure determined from extended Hückel-type calculations correlate well with the electrochemical results presented here ONLY when corrected for the effect of cumulative charging: Cain, S. R.; Gale, D. C.; Gaudiello, J. G., submitted for publication.

The electrochemical results presented here for the soluble polymer, when compared with those reported previously for the electrochemical oxidation of the insoluble analogue ($[Si(Pc)O]_n$), provide a basis for comparison between homogeneous (solution) and heterogeneous (solid-state) doping of a conductive system. Solid-state oxidation performed by either CPC on slurries or by electrochemical potential spectroscopy (ECPS) on microcompactions gave consistent results.[10m] The initial oxidation of the neutral virgin polymer is accompanied by a large overpotential associated with an irreversible first-order structural change. The resulting materials can then be doped and undoped over a wide potential, not unlike that reported here for the soluble polymer (Figure 2). ECPS results with a variety of anions illustrate that the maximum doping stoichiometries achievable are dictated mainly by anion size. Until the maximum doping level is approached, 67% for the mostly highly doped system, the percent oxidation vs potential profile is independent of the nature of the anion. The degree of oxidation at a given potential for the solid-state doping is nearly identical with that observed for the soluble polymer. This suggests that the data obtained from solid-state studies can accurately represent the inherent redox properties of conductive systems. These results also imply that the choice of counterion for solid-state doping is important and may limit the degree to which the material can be doped but not necessarily the potential at which doping occurs.

Conclusion

The electrochemical characterization of the soluble electrically conductive polymer μ-oxo-(tetra-*tert*-butylphthalocyaninato)silicon illustrates that the redox properties of conductive polymer systems can be accurately probed by conventional voltammetric techniques. Although a broad continuous redox response is observed, the standard potentials, diffusion coefficients, heterogeneous charge-transfer rates, and chemical stability of the system can be easily quantified. The percent oxidation vs potential profile for incremental doping can be quickly and precisely determined. Digital simulations of the observed voltammograms imply that the redox chemistry of conductive systems can be modeled as sequential electron transfer from an assembly composed of reversible redox couples. The simulated results allow a qualitative estimation of the degree of interaction between the redox centers.

Acknowledgment. We thank Professor Michael Hanack of the Institute for Organic Chemistry, University of Tubigen (Tubigen, FRG) for providing an improved synthesis for the precursors of the silicon polymer and Mark Cole (MSU) for running the mass spectrum of the monomer. The support of the Michigan State Center for Fundamental Materials Research and the donors of the Petroleum Research Fund, administered by the American Chemical Society, is gratefully acknowledged.